Materials and Design 65 (2015) 869–877

Contents lists available at ScienceDirect

Materials and Design

journal homepage: www.elsevier.com/locate/matdes

Thermal conductivity in yttria dispersed copper

Rajashekhara Shabadi [a,*], Marie Noëlle Avettand-Fènoël [a], Aude Simar [b], Roland Taillard [a], P.K. Jain [c], Roy Johnson [c]

[a] Unité Matériaux Et Transformations, UMR CNRS 8207, Université Lille – 1 Sciences et Technologies, France
[b] Institute of Mechanics, Materials and Civil Engineering, Université Catholique de Louvain, Louvain-la-Neuve, Belgium
[c] International Advanced Research Centre for Powder Metallurgy and New Materials (ARCI), Hyderabad 500 005, India

ARTICLE INFO

Article history:
Received 22 June 2014
Accepted 30 September 2014
Available online 14 October 2014

Keywords:
Oxide Dispersion Strengthened copper
Thermal conductivity
Grain size
Yttria
Recrystallization

ABSTRACT

The impact of yttria particles incorporated by Friction Stir Processing (FSP) on the thermal conductivity (TC) and Coefficient of Thermal Expansion (CTE) of copper is reported. Thermal properties of samples with or without powder were investigated for the temperature ranges between 40 and 240 °C as a function of the number of FSP passes. The reduction of CTE in the samples without powder is attributed to the decrease of the grain size during FSP. CTE values are rather close at the lower temperatures i.e., 40–80 °C, but, as the temperature rises to higher values there is a clear distinction between pure copper and samples with a modified microstructure. An impressive 27% reduction in the CTE was observed for a sample with uniformly distributed yttria particles in copper (i.e.; 9 passes with yttria) in comparison to pure copper. Thermal conductivity at 240 °C are slightly higher for the copper modified 3 passes and 9 passes with yttria powder when compared to pure copper. It was found that distribution of yttria particles in the copper matrix play a significant role in stabilizing the microstructure and hence reduce the CTE with no loss in thermal conducting ability of copper.

1. Introduction

Gas turbines, rocket nozzles, combustion chamber liners, combustor walls and rotating neutron target [1–5] require materials with high thermal conductivity (TC) in combination with elevated high temperature strength in oxygen or hydrogen environments. Copper is a natural choice thanks to its high thermal conductivity, low elastic modulus which reduces the thermal stresses, which are necessary characteristics of an actively cooled component. However, copper suffers from a large Coefficient of Thermal Expansion (CTE) and a reduction in high temperature strength as a result of recrystallization [6–8]. Hence, limiting the thermal expansion of copper is highly desirable as a first step to increase its applicability for thermal management applications. There are number of studies discussing the thermal stability of the microstructure of fine, deformed and severe plastically deformed copper [9–14]. However, there are very few reports concerning the thermal expansion of copper. One way of reducing the thermal expansion in pure metals is through the addition of oxide particles which impede the matrix from expansion under influence of the heat by forming pinning agents limiting the migration of the grain boundaries. This led to the development of Oxide Dispersion Strengthened (ODS) materials [15]. However, presence of such oxide particles could alter the thermal conduction by forming the scattering points for phonon conduction [16].

The question of the strengthening particle selection has been reviewed by Groza and Gibeling [17]. As per the different criterions considered by Groza and Gibeling [17] yttria tops all the tables with better physical properties and better thermodynamic stability in comparison to its counterparts such as Al_2O_3 [18–20], and SiC [21–23]. However, there are only few attempts [24–26] in the literature reporting successful dispersion of yttria in copper. Nagorka et al. [24] studied the feasibility of yttria dispersed copper using internal oxidation of rapidly solidified Cu–Y alloys. They prepared Cu–1 at%Y_2O_3 alloys using different processes such as conventional solidification, gas atomisation and splat-quenching. Of all the processes studied, splat quenched Cu–1 at% Y_2O_3 exhibited the better distribution of yttria particles after internal oxidation at 873 or 1123 K. Whereas in the other processes, the yttria particles were inhomogenously distributed due to interdendritic segregation. Zhuo et al. [26] prepared a Cu–0.4 wt% Y ODS alloy by in-situ reaction at the liquidus temperature (1070 °C), under an oxygen partial pressure of 2.1×10^{-3} Pa. They concluded that maintaining the alloy at the ideal liquidus temperature is critical in order to have

* Corresponding author at: Unité Matériaux Et Transformations, UFR de Chimie, UMR CNRS 8207, Bâtiment C6, 2eme étage, Université Lille – 1 Sciences et Technologies, 59655 Villeneuve d'Ascq, France. Tel.: +33 (0)320436224; fax: +33 (0)320434040.
E-mail address: Rajashekhara.Shabadi@univ-lille1.fr (R. Shabadi).

http://dx.doi.org/10.1016/j.matdes.2014.09.083
0261-3069/

uniform oxidation of yttrium to form finely distributed yttria in the matrix. They observed that the strength levels increased ~2.5 times after the internal oxidation procedure and attributed this strength levels to the grain refinement and also to the Orowan mechanism caused by the fine scale oxidation of yttrium (average 5 nm) in the matrix. The main problem with the internal oxidation is that of optimizing the process parameters affected by the slight variation in the alloy composition. Further, the size of the treated component is limited.

The present authors proposed to use [27] Friction Stir Processing (FSP) for incorporating yttria in copper. It has been shown that the processing parameters affect the grain size and the particle distribution in turn impacting the mechanical properties.

These works explore the possibilities of yttria dispersions in copper and its strengthening mechanisms. However, the production of such materials for thermal management applications is not addressed in the case of yttria dispersed copper. Fathy and El-Kady [19] studied the thermal conductivity (TC) of a thermomechanically processed Cu–Al_2O_3 composites (0–12.5%Al_2O_3). As expected, with the high content of Al_2O_3 there was a strong reduction (−75%) in the thermal conductivity of the composite as a result of differences in the way the heat conducts in ceramics and metals. The high volume fraction of Al_2O_3 acted as phonon scatterers to the smooth conduction of heat in the copper matrix. Hence, ODS copper, with a lower volume fraction is expected to be an ideal material to reduce the thermal expansion coefficient while keeping its thermal conductivity intact. The current work presents a conception and design of yttria dispersed copper with the use of FSP to improve the thermal properties of copper.

2. Materials and methods

2.1. Materials

Copper Cu-a1(Cu-ETP according to ISO 431 [28] and 1337 [29] standards) material in the H12 state was used for obtaining the ODS copper using FSP. The Cu-a1 was a plate of 5 mm × 195 mm × 46 mm (thickness × length × width) in which, symmetrical V-grooves of depth 0.75 mm, length 125 mm and the width 1.5 mm were carved at 1 mm on each side of the centerline of the plate. These grooves were compactly filled with yttria powders and finally the plate was covered with a 0.2 mm thick sheet of Cu-a1 (identical to the base material) to protect the powder from falling off during the FSP process. All of this assembly was finally placed on a backing plate (80 mm thick) made up of high carbon steel and the whole assembly was clamped on a work bench (Fig. 1).

2.2. Friction Stir Processing (FSP)

Above said set up was processed by FSP tool made up of tool steel. Tool tip was a Triflat pin (6 mm Ø, 3 mm in length) with M6 type threads on it. This pin is an extension of a shoulder of a 20 mm Ø with a spiral grooves on the shoulder surface (see Fig. 1 of Jonckheere et al. [30] for a full scheme of the tool geometry). The tool was inclined backwards by 1° so as to facilitate the easy passage of the material into the tool shoulder without tearing of the 0.2 mm thick cover sheet ahead of the tool. Table 1

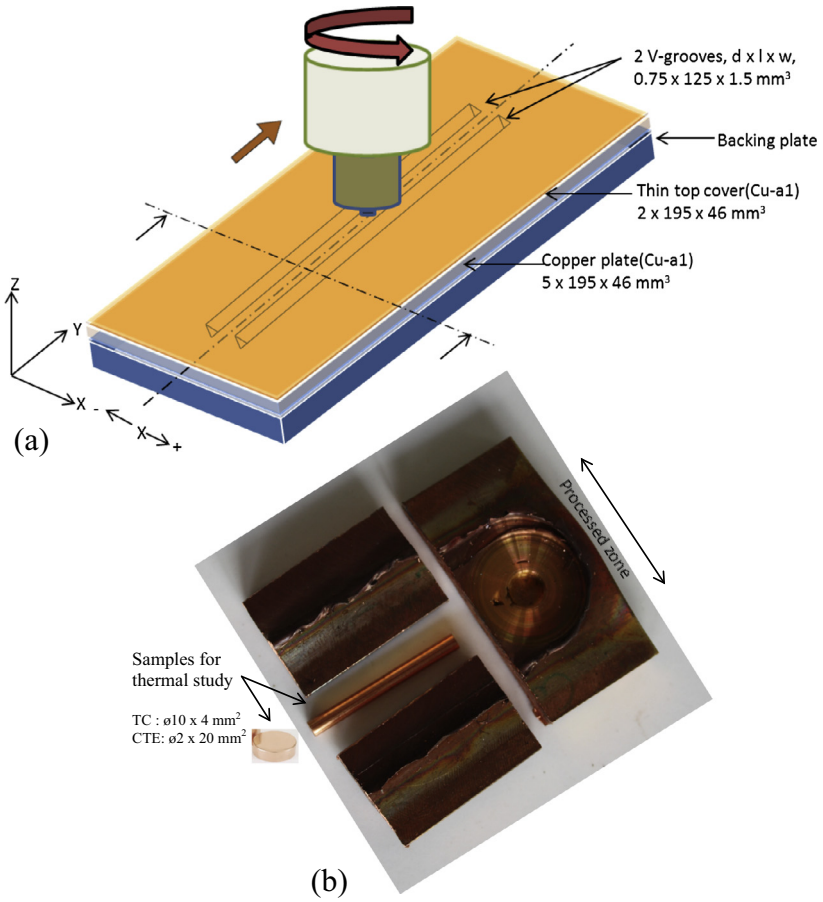

Fig. 1. Schematic of the samples processed with the Friction Stir Processing tool. (a) General assembly and (b) location of the samples studied.

Table 1
Process parameters of different samples using Friction Stir Processing.

Sample	Pass number	Locations of passes	
		Z (mm)	X (mm)
Cu plate	–	–	–
Cu 3 passes	1	−3.5	0
	2	−3.6	−1.5
	3	−3.7	+1.5
Cu + yttria 3 passes	1	−3.5	0
	2	−3.6	−1.5
	3	−3.7	+1.5
Cu 9 passes	1	−3.5	0
	2	−3.6	−1.5
	3	−3.7	+1.5
	4	−3.8	0
	5	−3.9	−1.5
	6	−4.0	+1.5
	7	−4.1	0
	8	−4.2	−1.5
	9	−4.3	+1.5
Cu + yttria 9 passes	1	−3.5	0
	2	−3.6	−1.5
	3	−3.7	+1.5
	4	−3.8	0
	5	−3.9	−1.5
	6	−4.0	+1.5
	7	−4.1	0
	8	−4.2	−1.5
	9	−4.3	+1.5

summarizes the different processing parameters used to obtain the samples with Friction Stir Processing. All the samples were processed with an advancing speed of 40 mm/min and with a rotating speed of 500 rpm. The tool penetration depth was maintained for a given pass and increased by 0.1 mm per pass. Copper with and without yttria powder were processed with 3 or 9 passes. For more details on the processing parameters readers are invited to consult Avettand et al. [27].

2.3. Sampling and orientation

After processing the samples using the FSP tool, test samples were taken from the processed zone. These grooves with powder were completely filled up after processing. The dotted line in Fig. 1a schematically indicates the place where the samples were cut for the material characterization purposes. All other samples were taken from the processed zone as indicated in Fig. 1b.

2.4. Material characterization

2.4.1. Microstructure

Microstructures of the processed zone were studied in the samples cut in transverse direction to the processing line as indicated in Fig. 1a. An in-depth study was undertaken to understand the microstructural features using an optical microscope and transmission electron microscopes (TEM). Heat treating a sample by rising it to 200 °C followed by quenching in water was carried out in order to study the microstructural changes under the influence of temperature. The choice of 200 °C corresponds to the exothermic peaks that are measured during Differential Scanning Calorimetry (DSC). After standard polishing, the metallographic surfaces were electrolytically polished and etched using 70% Orthophosphoric acid in demineralized water maintained at 10 °C using 2 V for 1–2 min and 0.5 V for 20–25 s respectively for polishing and etching.

For TEM, a thin slice ~300 μm was cut from the transverse section to the processing direction and mechanically thinned down to ~60 μm. Subsequently, it was electrochemically thinned down to make it electron transparent using Tenupol twin jet electrolytic polishing unit. The electrolyte was a 40% Orthophosphoric acid in demineralized water maintained at 10 °C at 2 V. A carbon coated copper grid was used to study the morphology of yttria particles. A small quantity of yttria powder was dissolved in ethanol and drop from it was deposited on the copper grid with a carbon layer. After degassing to completely evaporate the ethanol, the grid was used for the TEM analysis. Tecnai G20 operating at 200 KV was used for the TEM observations.

2.4.2. Thermal conductivity (TC)

TC was calculated using Eq. (1) mentioned below. Thermal diffusivity (α) measurements were carried out using laser flash technique (Netzsch LFA-427) on the samples taken from the processing zone as indicated in Fig. 1b were of 10 mm Ø and 4 mm thickness. Thermal diffusivity was measured from the ambient temperature to 240 °C. TC is related to the diffusivity through the following relation:

$$\alpha = \frac{k}{\rho . c_p} \tag{1}$$

where k is the thermal conductivity (W/m K), ρ is the density (kg/m^3) and c_p is the specific heat capacity (J/kg K). $\rho.c_p$ together, can be considered as the volumetric heat capacity (J/m^3 K). Thermal diffusivity measurements were with the precision of ±0.02–0.05 cm^2/s.

2.4.3. Differential Scanning Calorimetry

Differential Scanning Calorimetry (DSC) was used to follow the change in microstructure as a function of the rise in the temperature. A small quantity (~20 mg) in the form of 3 mm discs were punched out from the thin slice of the samples cut in the transverse direction. Hence, the size and the morphology of the samples used for DSC were constant for all the samples. DSC signal was recorded up to a temperature of 450 °C at a rate of 5 K/min.

2.4.4. Coefficient of Thermal Expansion (CTE)

CTE measurements were carried out on the samples taken from the processed zone (Fig. 1b). Samples were 2.5 mm Ø and 20 mm in length. The samples were subjected to the dilatometric analysis using Netzsch-402C dilatometer, scanned between room temperature and 240 °C at a heating rate of 5 K/min under argon atmosphere.

3. Results

3.1. Constituent materials and microstructure

Yttria particles used in the present study have an average size of 3.5 μm and have an irregular shape, see Fig. 2a. One of the particles was observed by TEM at a close up, it consists of nano grains of yttria with an average size of 10 nm, see Fig. 2b. The crystalline nature of the different grains are evidenced from planes observed in the grains of yttria, this is however not further explored as this is not the scope of the present study.

Fig. 3a presents the microstructure of the as received copper. Cu-a1 is a commercially available oxygen free high purity copper. Fig. 4 summarizes the mean grain sizes measured from different images. The microstructure shows the grains with lots of twins as typically observed in copper [10]. The mean grain size is equal to 35 μm. Fig. 3b shows the effect of the 200 °C heat treatment on the as-received copper. It has increased the grain sizes to more than 80 μm as a result of recrystallization. Fig. 3c, represent the microstructure of the 3 passes without the yttria and an average grain size of around 17 μm is observed. With the addition of the yttria particles, the same number of passes interestingly reduced

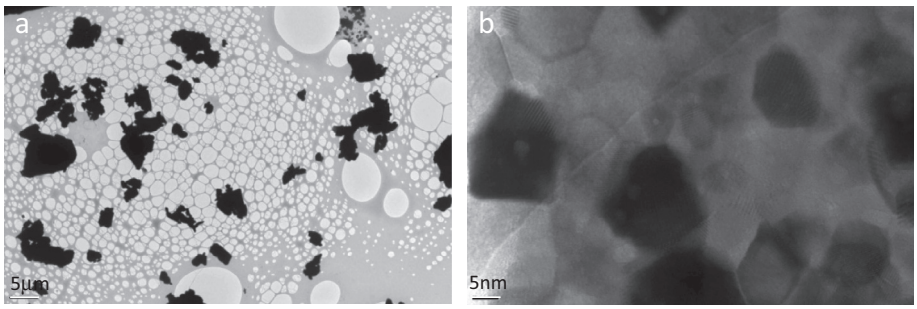

Fig. 2. Transmission Electron Microscopy of the (a) yttria particles and (b) Inner grain of a yttria particle.

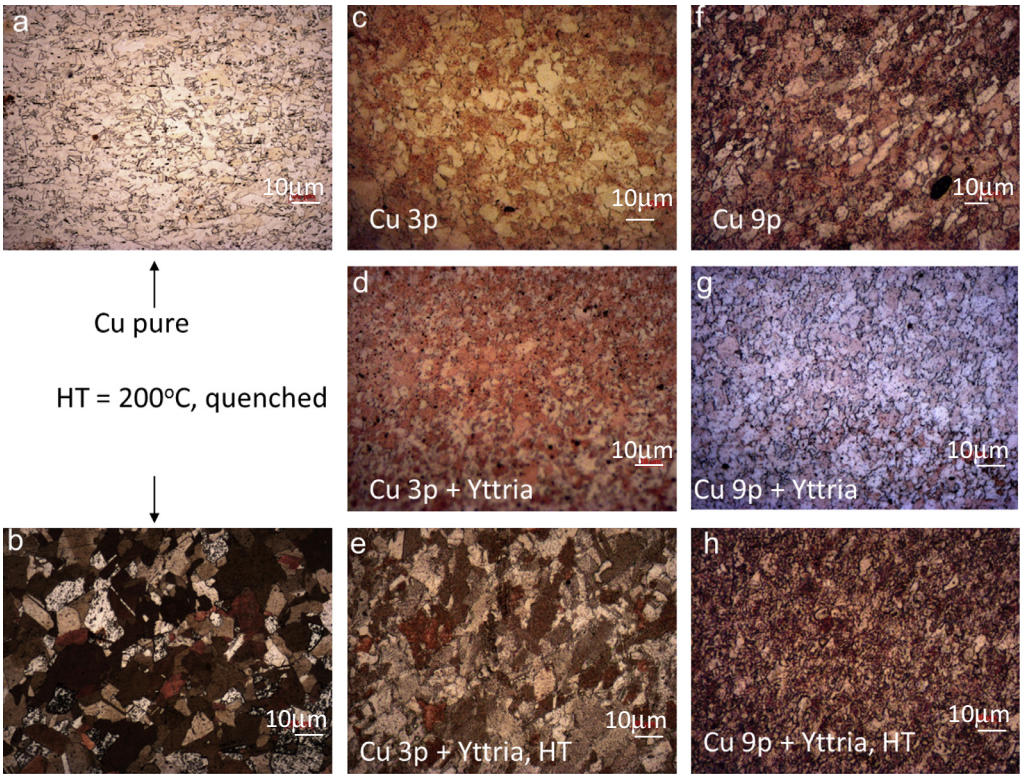

Fig. 3. Optical Micrographs of the processed zone of different FSP samples. (a) Cu as received, (b) Cu after heat treatment at 200 °C. (c) Cu 3 passes (d) Cu 3 pass + yttria (e) Cu 3 pass + yttria Heat treatment at 200 °C (f) Cu 9 passes (g) Cu 9 pass + yttria (h) Cu 9 pass + yttria, Heat treatment at 200 °C.

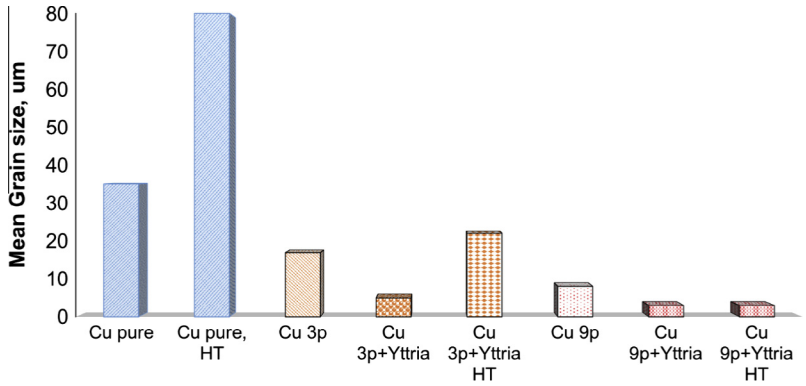

Fig. 4. Summary of the grain sizes measured in different materials.

the grain sizes to the levels of 5 μm, Fig. 3d. However, after the heat treatment at 200 °C, there was notable grain growth (22 μm) in the yttria containing 3 pass sample Fig. 3e. Increasing the number of passes to 9 on the copper plate further reduced the grain sizes to 8 μm. Addition of the yttria particles and the 9 passes further brought down the grain size to 3 μm. Interestingly,

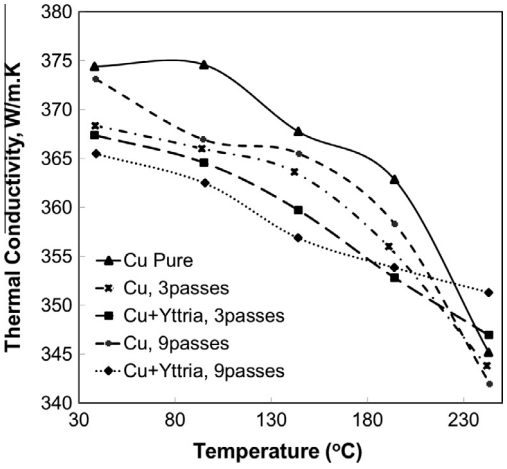

Fig. 5. Thermal conductivity measurements derived from the thermal diffusivity data (Eq. (1)) for different samples processed using FSP.

the heat treatment did not alter the grain size for the 9 pass sample.

3.2. Thermal Behavior of different materials

Fig. 5 presents the thermal conductivity (TC) calculated using Eq. (1). The as-received copper sample exhibits a TC of 374 W/m K which is very close to the values reported in literature that vary between 370 and 400 W/m K depending on the purity and the oxygen content [31]. Of all the materials studied, the lowest TC is that of the 9 pass with yttria powder having a TC equal to 365 W/m K. Fig. 5 evidences that every material exhibits a decreasing TC with the increasing temperature. However, yttria containing samples exhibit a difference at which the decrement occurs. Close to 200 °C, it appears there is a rapid decrease for all other materials except for the Cu + yttria 3 passes sample and an even lower decreasing rate is observed for Cu + yttria 9 passes sample. At 240 °C, the Cu + yttria 9 passes sample has a higher TC than any of the other materials studied. Table 2 summarizes the TC and CTE behavior at 240 °C for the comparative purposes.

Differential scanning calorimetry (DSC) measurements were carried out in order to find out the reason for the change in the TC slope at 200 °C. The DSC curves in Fig. 6 presents an exothermic peak for each of the FSPed samples studied approximately around 195 °C which corresponds to the recrystallization temperatures of a heavily deformed copper [14], whereas for the as-received copper the exothermic peak is found at 216 °C. All the DSC curves exhibit clear peaks except the curve of Cu + yttria with 9 passes which appeared to be more slowly declining after the peak observed at 195 °C. It is also worth noting that the deformation induced by the number of passes has an influence on the onset of recrystallization. It reduced the onset temperature of pure copper from 170 °C to 137–140 °C in the FSPed samples.

Fig. 7a represents the global view of the Coefficient of Thermal Expansion (CTE) as registered from dilatometry. Fig. 7b, is a magnified view of the range of 80–240 °C to clearly distinguish the curves.

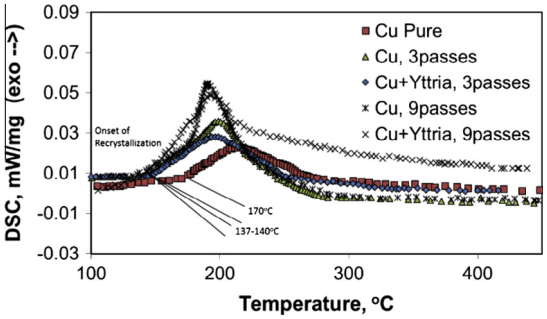

Fig. 6. Differential Scanning Calorimetry (DSC) of different samples studied.

Starting at room temperature (20 °C), the CTE remained more or less the same for all the samples. A clear evidence of deviation in the thermal expansion behavior could be noticed once the samples reach 80 °C. At 80 °C, the as-received copper has a CTE higher than the Cu + yttria with 9 passes. The absolute difference in CTE keeps on increasing until the end of the temperature range studied here. At 240 °C, the as-received copper has a CTE 27% higher than Cu + yttria with 9 passes. CTE of the samples with or without yttria follow a similar trend but the copper without yttria expand a little more with temperature than with the yttria powder (~2.5% difference at 240 °C). However, the samples with and without yttria for 9 passes demonstrated larger differences after 140 °C and toward 240 °C the CTE was 5% lower for the yttria containing samples.

3.3. Transmission Electron Microscopy

Fig. 8 represents a montage of the in-depth view of 3 passes and 9 passes samples with yttria powder before and after the 200 °C heat treatment. From the DSC analysis, it has been found that there is an exothermic peak at around 194–216 °C for all the samples. Hence, the samples were heat treated up to 200 °C and quenched immediately in water to preserve the microstructure. Fig. 8a presents the microstructure of 3 passes yttria containing sample of the as processed sample (without heat treatment). It can be seen that the grain sizes are approximately in agreement with the optical microscope observations (~3.5–5 μm) and present a lot of dislocation contrast. White spots on the image corresponds to agglomerates of yttria particles fallen out during the electrolytic thinning process. One such agglomerate of yttria in the 3 pass + yttria sample after heat treatment is observed in Fig. 8b. Fig. 8d corresponds to the 9 pass + yttria containing sample. From the image it can be observed that the grain sizes (~0.5–3 μm) are much smaller than that of 3 pass yttria containing sample and also with a lot more dislocation densities. Fig. 8e represents a typical image exemplifying the distribution of the yttria particles in the 9 pass + yttria sample. It can be seen that the distribution of the particles is more uniform in 9 pass sample compared to the 3 pass sample. Fig. 8c presents the microstructure of the 3 pass yttria containing sample after the heat treatment. The image reveals that after the heat treatment the grain sizes are much larger and also the dislocations disappeared from the grains. However, the same heat treatment in 9 pass yttria containing sample did not alter much the grain sizes (~0.5–3 μm) as observed from Fig. 8f. It

Table 2
Summary of the CTE at 240 °C for different materials.

Material	CTE (10^{-6}/K)	% CTE change w.r.t Cu pure	TC, W/m K	% TC change w.r.t Cu pure
Cu Pure	39.0	0	345	0
Cu 3 passes	36.2	7.2	343	−0.6
Cu + yttria 3 passes	35.3	9.5	347	+0.6
Cu 9 passes	30.1	22.8	341	−1.2
Cu + yttria 9 passes	28.6	26.6	352	+2.0

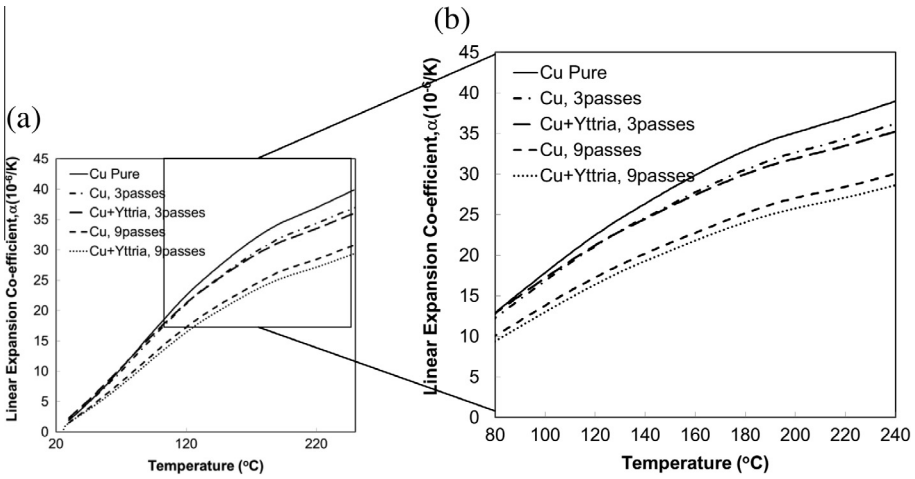

Fig. 7. Thermal expansion behavior of the different samples processed using FSP, (a) complete test, and (b) magnified view between 80 °C and 240 °C.

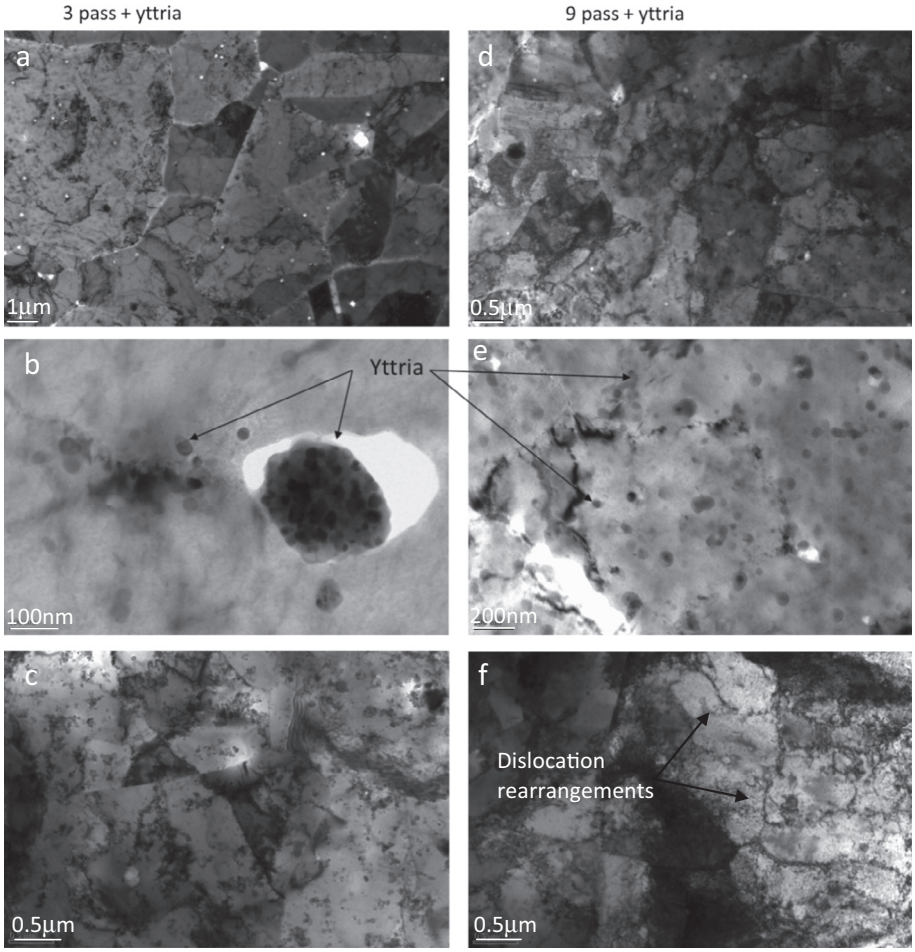

Fig. 8. Transmission Electron Micrographs of the core in the processed zone for different samples processed using FSP: (a) 3 pass + yttria as processed (b and c) 3 pass + yttria after heat treatment (d) 9 pass + yttria as processed (e and f) 9 pass + yttria after heat treatment.

appears that there are slight re-arrangements in the dislocation structure indicating a possible recovery in the microstructure.

3.4. Role of yttria particles in copper matrix

Yttria particles appear to play an important role in the grain boundary migration. Indeed, Fig. 9a presents an yttria particle pinning down the grain boundary. Yttria particles have been incorporated without much defects in the copper matrix as can be observed in Fig. 9b. The interface between the particle and the copper matrix is quite clean and no defects are observed.

4. Discussion

FSP was successfully employed to incorporate yttria particles in copper. Although the size of the ODS copper processed using FSP is

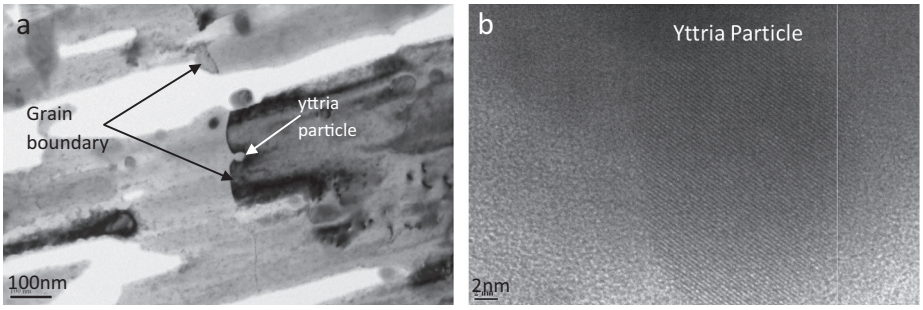

Fig. 9. Role of yttria particles in the copper matrix, in a 9 pass + yttria sample after heat treatment (a) grain boundary pinning, and (b) well integrated particle in the matrix.

only a couple of centimeters in the present study, it can easily be extended to larger sizes with suitable scaling up of the work table and the tool head machinery.

4.1. Microstructure

Fig. 3 and 4 summarize the effect of Friction Stir Processing and the heat treatment on the grain size evolution. As rolled copper microstructure (Fig. 3a) showed a massive increase in the grain sizes upon heat treatment at 200 °C as it lacked any grain boundary pinning agents (Fig. 3b). Fig. 3f shows a significant increase in the grain size (~22 μm) after the heat treatment at 200 °C from the as processed grain size which is around ~5 μm for the 3 passes + yttria sample. Whereas, the 9 passes + yttria sample did not show any change in the microstructure even after the 200 °C heat treatment (compare Fig. 3g and h). In 9 pass without yttria powder, it appears that a certain dynamic recrystallization occurred as evidenced by slightly bigger grains observed from Fig. 3f.

From Fig. 6, it can be noted that for the as received Copper, an exothermic peak appears at 216 °C resulting from a possible recrystallization of the rolled sheets. This temperature is in approximate agreement with the values observed elsewhere [12,13]. Although, the stored energy levels are not quantified in the present study, its intensity is much smaller when compared to the other FSPed samples which is concomitant with the fact that a heavily deformed material has more stored energy and will recrystallize more rapidly than a coarse grained material [6,10,12,14]. Which also explains the reduction of the onset temperature from 170 °C for pure copper to the 137–140 °C in the FSPed samples. Indeed, grain boundaries and excessive forest of dislocations are favorable nucleation sites for recrystallization. Accordingly, with increment in the number of passes, the reduction in recrystallization temperature is observed (170 °C to 137–140 °C), Fig. 6. Zhang et al. [13] reported a dramatic reduction in the recrystallization temperatures in their work on 99.98% pure copper using Equal Channel Angular Pressing (ECAP) to induce large deformations in the material. They reported a decrease of ~50 °C for the heavily deformed copper and stabilizing after 8 or more ECAP passes [13]. In the present study, a difference of nearly 30–33 °C is observed which is concomitant with the fact that the increasing deformation caused by the increasing number of FSP tool passes decreased the recrystallization temperature. It is also worth noting that the recrystallization process in not completed for the 9 pass + yttria containing sample as evidenced by the gradual decrease in the curve after hitting the peak at around 194 °C, Fig. 6. Plausibly indicating that the uniform distribution of the yttria particles are efficiently hindering the grain boundary migration and hence delaying the recrystallization phenomenon.

It is well known that, during the severe plastic deformations of metallic materials containing particles, the particles can influence in three ways the recrystallization of the matrix materials [6,32,33]. One is by increasing the stored energy in the matrix thereby facilitating the recrystallization. Second is by the creation of deformation heterogeneities at the vicinity of the larger particles which act as the nucleation sites for the recrystallized grains, which is popularly known as Particle Stimulated Nucleation (PSN). The third influence, is through their action as pinning agents for the grain boundary migration thereby retarding the grain growth. PSN is observed both in static recrystallization [6,32] and dynamic recrystallization[20,23,34] in particles containing metal matrix materials. The agglomerates of yttria particles (~200 nm Fig. 8b and even larger as observed in the white spots in Fig. 8a) for the lower number of passes i.e. 3 pass + yttria, act as nucleation sites and hence the fully recrystallized grains observed in Fig. 8c. Looking at the heat treated samples in TEM there are evidences to indicate that there are many instances of PSN in the 3 pass + yttria material. One such example is presented in Fig. 8b, wherein a big yttria agglomerate in the center of a newly recrystallized grain. Elsewhere, Humphreys and Ardakani [20] reported in Al_2O_3 and SiO_2 containing copper the influence of the size of the particles in particles on recrystallization. Sun and Fujii [23] reported the effect of SiC particles on the recrystallization of Copper in their recent study. These studies clearly indicated bigger particles tend to increase the PSN phenomenon. However, much finer disintegration of the yttria powder as a result of repeated attrition by the FSP tool into individual yttria crystals of an average size ~10 nm resulted in a more stable microstructure as in the case of 9 pass + yttria, while nanometric yttria acting as grain boundary pinning agents (Fig. 9a). Hence, the 9 pass + yttria sample presents more hindrances for the grain boundary migration and recrystallization at 200 °C. Finer distribution of the particles leads to the stable microstructure as evidenced elsewhere in a recent study by Shen et al. [34]. They studied the stability of fine grained copper with the dispersion of Al_2O_3 particles and concluded that the mechanical properties of the Cu–0.23 wt% Al_2O_3 were much better than that of the pure oxygen free high purity copper as a result of the increased stability of the microstructure in presence of the Al_2O_3 particles. Fig. 9a, represents one such image where an yttria particle effectively hindering the grain boundary migration. An increased number of passes also enhanced the interface contact between the yttria and the copper matrix, Fig. 9b is an example of homogeneous incorporation of the particle into the matrix.

4.2. Thermal conductivity (TC) and Co-efficient of Thermal Expansion (CTE)

TC is obtained through experimental evaluation of the thermal diffusivity of each material between the temperature ranges 40–240 °C. Reduction in the TC at 40 °C (Fig. 5) of the FSPed samples can be correlated to the deformed grains because of the repeated tool movement. This is in agreement with the fact that reduced grain sizes, increased dislocation density acts as the

scattering centers for the phonon conduction [16]. Decreasing trend in TC with the increasing measuring temperature TC is observed for all the samples studied in the present study. However, after around 200 °C the rate at which the TC decreased is more rapid many samples except for the 9 pass + yttria sample. A plausible explanation for this behavior could be found in the DSC curves represented in Fig. 6. Although the onset temperature for most of the deformed samples is around 137–140 °C there is an exothermic peak at around 194 °C which corresponds to the recrystallization temperature and this could a reason for a rapid decrease in the TC of most of the metals except the 9 pass + yttria containing sample. Again, referring to Fig. 6 the recrystallization curve for the 9 pass + yttria, which indicates a slow tail after the peak could easily be correlated to the microstructural stability brought in by efficient grain boundary pinning that is imparted from the uniform dispersion of the yttria particles in 9 pass + yttria samples. Recrystallization in turn is a result of relaxation of the stored energy and the dislocation re-arrangement that leads to the newly created grains. In the present study it is observed that, with the decreasing dislocation density and subsequent recrystallization of the instable microstructure (as in the case of pure copper, 3 passes and 9 passes without yttria) TC decreased rapidly than for the samples containing yttria with 3 passes and 9 passes. From Fig. 4, it can be seen that the grain size of the 3 pass + yttria containing sample had a substantial increase in the grain size after the heat treatment at 200 °C for 1hr. At the same time, TC for the same sample showed lesser slope at these temperatures, Fig. 5. This aspect indicates that the recrystallized and defect free grains are favorable for the thermal conductivity. However, a stable microstructure with the presence of grain boundary pinning agent (i.e. 9 pass + yttria samples) leads to a TC more or less reaching a plateau beyond 200 °C. Recent works on gold nanowires [35,36] and dense ceramic materials [37] have demonstrated that the deviations of electrical and thermal conductivities from the respective bulk properties are primarily related to the electron scattering at the grain boundary dislocations. It has also been stated that there is an inverse dependence of TC on the dislocation density as they constitute thermal resistance. The authors are not aware of any independent experimental evidence that correlates the dislocation density to the thermal conductivity.

Further, it is well known that the conduction in metallic materials is a combination of electron and phonon conductivities. These are limited by various scattering mechanisms which will give rise to the thermal resistance. In pure metals, conduction by phonons is usually quite small and is easily neglected because it is contribution is less than 5% at 100 K and even lesser at higher temperatures [38]. However, contribution from phonon cannot be neglected in the case of heavily alloyed and/or heavily deformed materials [39]. Initial reduction in the thermal conduction in the deformed materials as in the case of the 3 pass and 9 pass with or without yttria can be explained by the increase of dislocations and the distorted lattice structure due the severe plastic deformation caused by the FSP tool. This lattice distortion and the reduction in the grain sizes cause hindrances to the electron phonon interaction and transfer of heat at the grain boundaries that act as the scatterers. Gendelman et al., reported this observation in their work on ECAP on copper samples and observed that with the increased ECAP passes grain size reduces and also the thermal conductivity measured using a stationary method [10]. However, further reduction in the thermal conductivities beyond 140 °C as the recovery and recrystallization sets in the material could not be explained at this point of time with the experimental methods employed in the present study. Or, it is also possible that further prolongation of the measurements of TC at higher temperatures might indicate a reversal of the phenomenon as clean/recrystallized/annealed microstructure is favorable for the thermal/electrical conductivity as proposed in a recent study, although that was in the case coatings [40]. Further, the reduction of TC in the samples containing yttria has in addition the influence of poor conductivity of ceramic particles.

Fig. 7a represents the global view of the Coefficient of Thermal Expansion (CTE) as registered from dilatometry. As evident from Fig. 7b, there is a clear distinction between the material behaviors. As received copper has the higher CTE as expected because of lack of grain growth hindering particles. Whereas, Cu + yttria with 9 passes sample exhibited a much lesser CTE when compared to any other sample studied. This reduction in CTE could be directly attributed to the finer distribution of the yttria particles and its efficiency in pinning the grain boundary migration as observed in Fig. 9a. An impressive gain of 27% reduction in CTE is achieved with the finer distribution of yttria in copper with 9 passes.

5. Conclusions

Effect of microstructural change brought by the FSP and presence of yttria particles on the thermal conductivity (TC) and Coefficient of Thermal Expansion (CTE) is discussed. Thermal properties have been studied at the temperature ranges between 40 and 240 °C, as a function of the number of passes with or without yttria particles. Mere modification of the base microstructure by FSP (without powder) reduces the CTE by 3.3–4.2% for 3 passes and 9 passes respectively at 40 °C. Reduction in the CTE in the samples without powder is attributed to the reduction in the grain size and the increased dislocations as a result of repeated deformation brought about by the FSP. Increased reduction in CTE with the inclusion of the oxide particles caused by the constraints exerted by the particle incorporation into the copper matrix which impede the expansion of the grains under the thermal influence. It is worthy to note that yttria particles have been completely dispersed and integrated well with in the copper matrix only at the larger number of FSP passes (i.e. 9 passes). CTE values are rather close at the lower temperatures i.e., 40–70 °C, but as the temperature rises to higher values, it is clear that the microstructure modified by the FSP plays an important role in the reduction of the CTE. At 240 °C, Cu + yttria with 9 passes exhibits a CTE 27% lower than the base Cu. TC appeared to be slightly higher for the copper samples modified by FSP without powder. Reduction in the TC with the temperature is observed for the samples without powder and approached the pure copper values at 240 °C. However, conductivity values were still on the higher side for the samples with the yttria and the major influence being the uniform distribution of the particles in the copper matrix thereby providing a stable microstructure.

Acknowledgements

A.S. acknowledges the financial support from the Interuniversity Attraction Poles Program from the Belgian State through the Belgian Policy Agency; contract IAP7/21 “INTEMATE”.

References

[1] Qin Jinggang, Wu Yu, Yu Min, Liu Bo, Liu Huajun, Weiss Klaus-Peter, et al. Manufacture of ITER feeder sample conductors. Fusion Eng Des 2013;88(9-10):1461–4.
[2] Agostinetti P, Dalla Palma M, Dal Bello S, Heinemann B, Nocentini R, Zauner C, et al. Investigation of the thermo-mechanical properties of electro-deposited copper for ITER. J Nucl Mater 2011;417(1-3):924–7.
[3] Rowcliffe AF, Zinkle SJ, Stubbins JF, Edwards DJ, Alexander DJ. Austenitic stainless steels and high strength copper alloys for fusion components. J Nucl Mater 1998;258–263:183–92.
[4] Davis JW, Kalinin GM. Material properties and design requirements for copper alloys used in ITER. J Nucl Mater 1998;258–263:323–8.
[5] Paton’ NE. Materials for advanced space propulsion systems’. Mater Sci Eng, A 1991;143:21–9.

[6] Benchabane G, Boumerzoug Z, Thibon I, Gloriant T. Recrystallization of pure copper investigated by calorimetry and microhardness. Mater Charact 2008;59:1425–8.
[7] Humphreys FJ, Hatherly M. Recrystallization and related annealing phenomena. 2nd ed. UK: Elsevier; 2004.
[8] Mao WM et al. Recrystallization and grain growth. Beijing: Publishing Company of Metallurgy Industry; 1994.
[9] Takata N, Yamada K, Ikeda K-I, Yoshida F, Nakashima H, Tsuji N. Change in microstructure and texture during annealing of pure copper heavily deformed by accumulative roll bonding. Mater Trans 2007;48(8):2043–8.
[10] Gendelman OV, Shapiro M, Estrin Y, Hellmig RJ, Lekhtmakher S. Grain size distribution and heat conductivity of copper processed by equal channel angular pressing. Mater Sci Eng, A 2006;434:88–94.
[11] Saldana C, King AH, Chandrasekar S. Thermal stability and strength of deformation microstructures in pure copper. Acta Mater 2012;60:4107–16.
[12] Li YS, Zhang Y, Tao NR, Lu K. Effect of the Zener–Hollomon parameter on the microstructures and mechanical properties of Cu subjected to plastic deformation. Acta Mater 2009;57:761–72.
[13] Zhang Y, Wang JT, Cheng C, Liu J. Stored energy and recrystallization temperature in high purity copper after equal channel angular pressing. J Mater Sci 2008;43:7326.
[14] Ridha AA, Hutchinson WB. Recrystallisation mechanisms and the origin of cube texture in copper. Acta Metall 1982;30(10):1929–39.
[15] Froes FH, de Barbadillo JJ, Suryanarayana C. Structural Applications of Mechanical Alloying. In: Froes, deBarbadillo, editors, vol. 1. ASM Intl.; 1990.
[16] Biswas K, He J, Blum ID, Wu C, Hogan TP, Seidman DN, et al. High-performance bulk thermoelectrics with all-scale hierarchical architectures. Nature 2012;489:414–8.
[17] Groza JR, Gibeling JC. Principles of particle selection for dispersion strengthened copper. Mater Sci Eng, A 1993;171:115–25.
[18] Rajkoci V, Bozic D, Jovanovic MT. Properties of copper matrix reinforced with various size and amount of Al_2O_3 particles. J Mater Process Technol 2008;200:106–14.
[19] Fathy A, El-Kady O. Processing, characterization and properties of copper-based composites strengthened by low amount of alumina particles. Mater Des 2013;46:355–9.
[20] Humphreys FJ, Ardakani MG. Grain boundary migration and Zener pinning in particle-containing copper crystals. Acta Mater 1996;44:2717–27.
[21] Akramifard HR, Shamanian M, Sabbaghian M, Esmailzadeh M. Microstructure and mechanical properties of Cu/SiC metal matrix composite fabricated via friction stir processing. Mater Des 2014;54:838–44.
[22] Akbarpour MR, Salahi E, Alikhani Hesari F, Yoon EY, Kim HS, Simchi A. 'Microstructural development and mechanical properties of nanostructured copper reinforced with SiC nanoparticles'. Mater Sci Eng, A 2013;568:33–9.
[23] Sun YF, Fujii H. The effect of SiC particles on the microstructure and mechanical properties of friction stir welded pure copper joints. Mater Sci Eng, A 2011;528:5470–5.
[24] Nagorka MS, Levi CG, Lucas GE. The potential of rapid solidification in oxide-dispersion-strengthened copper alloy development. Mater Sci Eng, A 1991;142:277–89.
[25] Nagorka MS, Levi CG, Lucas Glenn E. Novel oxide-dispersion-strengthened copper alloys from rapidly solidified precursors: Part 1. Microstructural development. Metall. Mater. Trans. A 1995;26A:859–71.
[26] Zhuo H, Tang J, Ye N. A novel approach for strengthening Cu–Y2O3 composites by in situ reaction at liquidus temperature. Mater Sci Eng, A 2013;584:1–6.
[27] Avettand-Fènoël M-N, Simar A, Shabadi R, Taillard R, de Meester B. Characterization of oxide dispersion strengthened copper based materials developed by friction stir processing. Mater Des 2014;60:343–57.
[28] ISO Standard 431. International Organization for Standardization; 1981.
[29] ISO Standard 1337. International Organization for Standardization; 1980.
[30] Jonckheere C, Meester B, Denquin A, Simar A. Torque, temperature and hardening precipitation evolution in dissimilar friction stir welds between 6061–T6 and 2014–T6 aluminum alloys. J Mater Proc Tech 2013;213:826–37.
[31] Powell RL, Roder HM, Rogers WM. Low temperature thermal conductivity of some commercial coppers. J Appl Phys 1957;28:1282–8.
[32] Doherty RD, Martin JW. The effect of a dispersed second phase on the recrystallization of aluminum–copper alloys. J Inst Met 1962;91:332.
[33] Goetz RL. Particle stimulated nucleation during dynamic recrystallization using a cellular automata model. Scripta Mater 2005;52:851–6.
[34] Shen K, Guo M, Wang M. Recrystallization characteristics of a fine grained copper alloy. Mater Chem Phys 2010;120:709–14.
[35] Wu W, Brongersma AH, Van Hove M, Maex K. Influence of surface and grain-boundary scattering on the resistivity of copper in reduced dimensions. Appl Phys Lett 2004;84:2838–40.
[36] Bietsch A, Michel B. Size and grain-boundary effects of a gold nanowire measured by conducting atomic force microscopy. Appl Phys Lett 2002;80:3346–8.
[37] Litovsky E, Shapiro M. Gas pressure and temperature dependences of thermal conductivity of porous ceramic materials: Part 1, refractories and ceramics with porosity below 30%. J Am Ceram Soc 1992;7:3425–39.
[38] Issi JP, Heremans J. Electronic and lattice contributions to the thermal conductivity of graphite intercalation compounds. Phys Rev B 1983;27:1333.
[39] Hamachiyo T, Ashida M, Hasezaki K. Thermal conductivity of Bi0.5Sb1.5Te3 affected by grain size and pores. J Electron Mater 2009;38:1048–51.
[40] Seo D, Ogawa K, Sakaguchi K, Miyamoto N, Tsuzuki Y. Influence of crystallite size and lattice spacing on thermal conduction of polycrystalline copper deposited by solid particle impingement: contribution of electron and phonon conduction. Surf Coat Tech 2012;207:233–9.